Climate Benchmarking Using GPS Occultation

Stephen S. Leroy, John A. Dykema, and James G. Anderson

Harvard University, Cambridge, Massachusetts, USA

Summary. Climate monitoring is of pre-eminent importance in this era of global change, and GPS occultation is an ideal technique for climate monitoring. We put climate monitoring in a scientific context, which can be arrived at through careful implementation of Bayesian inference. What we find is that a good climate monitoring tool must help address the physics of a climate model so as to make it better able to predict future climates. GPS occultation is ideal because it offers sensitivity to improve the model physics which affects the stratospheric Brewer-Dobson circulation, the tropical tropospheric hydrological cycle, and the poleward migration of the mid-latitude storm track. Also, GPS occultation is ideal because it can be readily made into a benchmark measurement provided clock calibration is always done by double-differencing, and measurements used to determine precise orbits and information on ionospheric activity are archived as auxiliary information. In doing so, GPS occultation can be made S.I. traceable.

The promise of radio occultation using the Global Positioning System as a climate monitoring technique has been recognized for a long time [1, 2, 3], but exactly how occultation data can be used for this purpose and why it might be appropriate to use radio occultation for climate monitoring has never been formalized. Certainly, radio occultation offers advantages over other sounding techniques which have been used in the past for climate monitoring, namely calibration using a time standard traceable to atomic clocks through double differencing (to be discussed later), but does radio occultation offer a guarantee of capturing the true state of the atmosphere? If GPS occultation is needed, what are the actual requirements for making it an essential climate monitoring tool?

The above questions on climate monitoring by GPS occultation can be answered by outlining a background to global climate change, describing how climate change research can be philosophically linked to climate monitoring, and defining the qualities of a measurement which makes it useful for climate monitoring. It is not in the scope of this work to discuss in any detail the background to climate change, and it is left to the reader to consult the

Third Assessment Report of the Intergovernmental Panel for Climate Change (IPCC2001) [4] for a thorough review of observations used to probe climate change over the past century. We will, however, discuss a philosophy which puts climate monitoring in a scientific context and assess the accuracy with which current GPS occultation must capture the true state of the climate.

1 An Overview of Climate Monitoring

The reason climate monitoring is of current interest is that global warming and the strong possibility that human activities are at least in part to blame has become a key scientific debate. In addition, any societal attempt to limit warming by greenhouse gas emissions in the future must be informed by reliable forecasts of climate change in the future.

That the surface air has been warming over the past century is very likely [5]. The warming has occured primarily in two intervals: one from 1910 through 1940, and the second from 1970 to the present. The temporal pattern is consistent with an atmospheric greenhouse instigated by increasing carbon dioxide, methane, nitrous oxide, and chloro-fluorocarbons. The absence of a trend between 1940 and 1970 is thought to be due to the presence of sulfate aerosols, which reflect shortwave radiation.

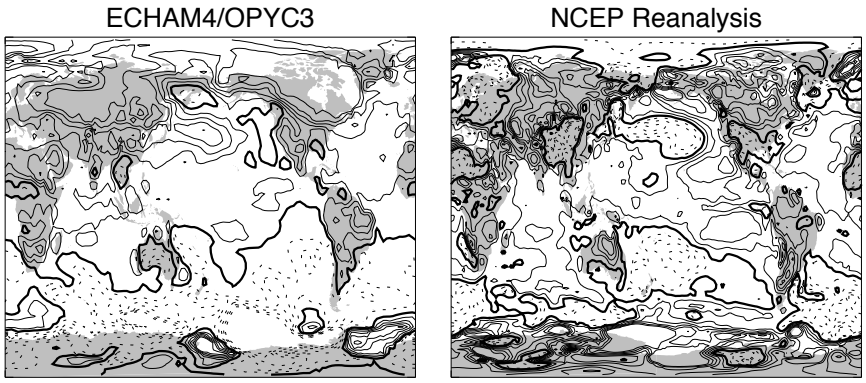

Fig. 1. Trend of 2-meter air temperature in ECHAM4/OPYC3 and the NCEP Reanalysis, 1970–1989. The left plot shows the temperature trend in the air temperature at 2 m above the surface as modeled by the ECHAM4/OPYC3 climate model with realistic greenhouse gas, sulfate aerosol, and ozone forcing. The plot on the right shows the same but taken from the NCEP Reanalysis. Each contour represents 0.2 K decade^{-1}. Solid (dashed) line contours are for positive (negative) values, and the thick line is the zero contour.

While it is possible to construct models of warming over the past few centuries that can match the temporal pattern of observed trends, there remain

substantial difficulties in modeling the spatial pattern of surface air temperature over recent decades. Fig. 1 shows the surface air warming trend in the climate model ECHAM4/OPYC3[1] for the period 1970 through 1989 in comparison with the NCEP Reanalysis [6]. Bulk features such as the relatively stronger warming over land versus over ocean are common to both model and reanalysis. Substantial differences over the ocean, especially the Pacific basin, however, reveal major difficulties in modeling change of the atmosphere's circulation. It is difficult to attribute the disagreement in southern high latitudes to the climate model or reanalysis, there being reasons to distrust both in this region. Detailed differences in trends over land are a consequence of the simplicity of land surface/biosphere parameterizations. The discrepencies in the spatial patern of surface air warming point to inadequacies in our ability to physically model the climate system.

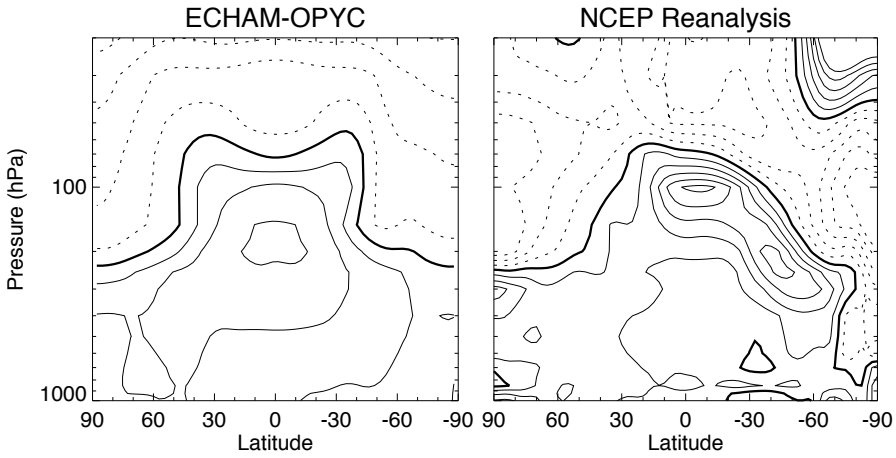

Fig. 2. Trends in upper air temperature in model and reanalysis due to increasing greenhouse gases, 1970–2000. The plot on the left shows the trend in upper air temperature as modeled by ECHAM4/OPYC3 when carbon dioxide increases at 1% year^{-1}. The plot on right shows the trend in upper air temperature from the NCEP Reanalysis from 1970 through 2000. Contour intervals are 0.2 K decade^{-1}. Solid (dashed) lines are for positive (negative) values, and the thick line is the the zero contour.

To further illustrate the point of difficulties in predicting atmospheric change, Fig. 2 shows patterns of upper air warming predicted to result from carbon dioxide increases. Upper air temperature trends predicted by the ECHAM4/OPYC3 model when it is subjected to a steady 1% yr^{-1} carbon

[1] The 2-m surface air temperature output from ECHAM4/OPYC3 was obtained from the on-line data gateway for the Third Assessment Report of the Intergovernmental Panel for Climate Change.

dioxide increase are compared to upper air temperature trends of the NCEP Reanalysis from 1970 through 2000. The comparison is reasonable because greenhouse gas increases dominate the tropospheric temperature trend from 1970 through 2000. Because the model forcing is not absolutely realistic in that it does not contain the right carbon dioxide forcing, ozone forcing, etc., we only concern ourselves with the overall patterns of warming exhibited. Of particular note is the lack of upper tropical tropospheric warming in the reanalysis in comparison to the model. Moreover, the strong warming lobe at the tropopause at the southern subtropical front is completely absent in the model prediction. Such effects are indications of the model's physics lacking the ability to adequately predict dynamical trends in the atmosphere. The consequences for the hydrological cycle are substantial.

The inadequate physics of the climate model is related to the uncertain model parameterizations pertaining to the hydrological cycle. For example, the water cycling rate and precipitation efficiency, two key parameters of the hydrological cycle, exhibit strong control over precipitation patterns in the tropics [7]. Atmospheric dynamics is governed by the equations of motion, which are explicitly integrated in an atmospheric model. Atmospheric motion is ultimately forced by external and internal heating due to radiation and latent heating. Because the dynamical evolution of water and clouds contribute to these heating effects on scales much smaller than the model resolves, they are parameterized. Such parameterizations, especially those pertaining to the hydrological cycle, are notoriously inadequate in simulating a realistic hydrological cycle.

What is needed is a methodology which relates climate monitoring to the scientific process wherein theories, or models, are tested against empirical data. By monitoring climate change carefully it is possible to reduce uncertainties in climate models, especially those pertaining to parameterizations, and thus make them more useful tools in forecasting climate change.

2 Bayesian Inference and Climate Signal Detection

A climate monitoring system must be reliable enough to help refine our capability of predicting future climate change [8]. This is the result when detecting climate signals by optimal fingerprinting is put into its Bayesian context [9].

In optimal fingerprinting, one searches for m climate signals with patterns $\mathbf{s}_i$, columns of $\mathbf{S}$, in an observational data set $\mathbf{d}$ with dimension n in the presence of naturally occuring variability $\mathbf{n}$. *A priori,* the amplitudes α_i of the signals are considered unknown. The patterns of the climate signals are expected to uniquely identify, or "fingerprint," the forcing which causes them. As such, this technique has been used in climate signal detection and attribution studies [10]. The model for the data is

$$\mathbf{d} = \mathbf{S}\alpha + \mathbf{n}. \tag{1}$$

In Bayesian statistics, the posterior knowledge for signal amplitudes given the data $p(\alpha|\mathbf{d})$ is proportional to the evidence for the data $P(\mathbf{d}|\alpha)$ multiplied by the prior for the signals' amplitudes $p(\alpha)$. All told,

$$p(\alpha|\mathbf{d}) \propto P(\mathbf{d}|\alpha)\ p(\alpha)$$
$$P(\mathbf{d}|\alpha) = (2\pi)^{-n/2}\,|\mathbf{N}|^{-1/2}\ \exp\Big[-\frac{1}{2}(\mathbf{d}-\mathbf{S}\alpha)^T\mathbf{N}^{-1}(\mathbf{d}-\mathbf{S}\alpha)\Big]. \qquad (2)$$

In optimal fingerprinting, the signal shapes, the interannual variability covariance $\mathbf{N}$ are considered known, no prior knowledge is considered, and the result is a probability distribution telling whether the consequences of specific forcings are detectable in the data.

This technique has been used to investigated the degree to which global warming can be attributed to human influences. Using models to formulate a distinctive pattern of temperature change caused by increasing greenhouse gases, it is possible to distinguish such a pattern from natural variations of the climate system. If successful, then warming of the surface air can be attributed to human influence. Significant problems remain with such an interpretation, though. Primarily, the detection of a human influence on climate is not the same as an attribution of global warming to human influence. For example, the overwhelming influence of carbon dioxide on atmospheric temperature is its cooling of the stratoshere. A complete implementation of optimal fingerprinting would appropriately lead to the conclusion that stratospheric cooling is the result of a human influence on climate. Although tropospheric warming may be part of that influence, it is inappropriate to conclude that tropospheric warming is a reliably detected result of human influence. The reason such a conclusion cannot be drawn is that the physics of stratospheric cooling differs radically from the physics of tropospheric warming.

A better way to implement Bayesian statistics is to recognize that neither the signal patterns nor their amplitudes are known *a priori*. These unknowns can be bundled into a package of uncertain parameters of a climate model, the source of our uncertainties in predicting climate change. (We assume strong knowledge of all external forcing of the atmosphere.) The coefficients of the model are μ, and the data $\mathbf{d}$ is modeled as

$$\mathbf{d} = \mathbf{f}(\mu) + \delta\mu \cdot \nabla_\mu \mathbf{f}(\mu) + \mathbf{n} \qquad (3)$$

where $\mathbf{f}$ is a kernel for how a signal is simulated by a model with parameters μ. For example, if the data represent the signal of the greenhouse effect as observed in radiosondes in the form of a trend, then $\mathbf{f}(\mu)$ is how a model predicts that trend would look given parameter values μ. The Jacobian $\nabla_\mu \mathbf{f}(\mu)$ tells how the trend would change by changing the parameters μ. If the prior for the model parameters is μ_0 with uncertainty covariance $\mathbf{\Sigma}_\mu$, i.e. $\mu \sim \mathcal{N}(\mu_0, \mathbf{\Sigma}_\mu)$,[2]

[2] A normal distribution can be written as $\mathbf{y} \sim \mathcal{N}(\mathbf{y}_0, \mathbf{Y})$ where the probability distribution for the n-dimensional vector $\mathbf{y}$ is $p(\mathbf{y}) = (2\pi)^{-n/2}\,|\mathbf{Y}|^{-1/2}\ \exp\big[-\frac{1}{2}(\mathbf{y}-\mathbf{y}_0)^T\mathbf{Y}^{-1}(\mathbf{y}-\mathbf{y}_0)\big]$.

then the Bayesian solution is $\mu \sim \mathcal{N}(\mu_{\rm mp}, \mathbf{\Sigma}_{\mu,\rm mp})$ where the "most probable" model parameters $\mu_{\rm mp}$ and their error covariance $\mathbf{\Sigma}_{\mu,\rm mp}$ are given by

$$\begin{aligned} \mu_{\rm mp} &= \mu_0 + \left((\nabla_\mu \mathbf{f})^T \mathbf{N}^{-1} (\nabla_\mu \mathbf{f}) + \mathbf{\Sigma}_\mu^{-1}\right)^{-1} \\ &\quad (\nabla_\mu \mathbf{f})^T \mathbf{N}^{-1} (\mathbf{d} - \mathbf{f}(\mu_0)) \\ \mathbf{\Sigma}_{\mu,\rm mp} &= \left((\nabla_\mu \mathbf{f})^T \mathbf{N}^{-1} (\nabla_\mu \mathbf{f}) + \mathbf{\Sigma}_\mu^{-1}\right)^{-1}. \end{aligned} \tag{4}$$

The Jacobian $\nabla_\mu \mathbf{f}$ is evaluated with parameters $\mu = \mu_0$ using several runs of a climate model, at least two runs for every parameter in μ. (Should a climate adjoint be constructed, only two runs of the climate model would be necessary.)

Eqs. 4 show how to improve a model using Bayesian inference. Using a climate data set which contains information on how highly uncertain components of the climate system respond to a known forcing over the duration of the data, one can tune the parameters of the model so that it responds in the same way as observed. This type of analysis has been implemented using surface air temperature data over the past century to estimate oceanic parameters but with limited success [11].

3 Climate Model Uncertainties and How They are Realized in Microwave Refractivity

So what are the implications for GPS radio occultation? That GPS occultation can be used for climate monitoring has been mentioned elsewhere, but the requirements that entails have never been formalized. Climate model improvement by detecting the emergence of responses to external forcing provides the theoretical framework for deducing requirements for climate monitoring.

To implement Bayesian inference as described above, one must assess the influence on climatic trends as produced by changing each of a model's least constrained parameters. This is an expensive proposition (but one that has been undertaken by `climateprediction.net`). A simple way around this computational expense is to assume instead that the world's premier climate models differ in their responses to a prescribed forcing in ways that reflect what happens when the parameters within any given model are adjusted within reason. By examining the differences between different models' predictions of future climatic trends given a prescribed forcing, we can deduce what information GPS occultation provides in improving model predictive capability.

We use the ensemble of climate models which contributed to the Coupled Model Intercomparison Project (CMIP2+) [12]. We chose to work with output of the models which provided temperature, humidity, and height on pressure surfaces, namely the German MPI Hamburg model (ECHAM4/OPYC3); the British Hadley Centre models (HadCM2, HadCM3); the Australian CSIRO

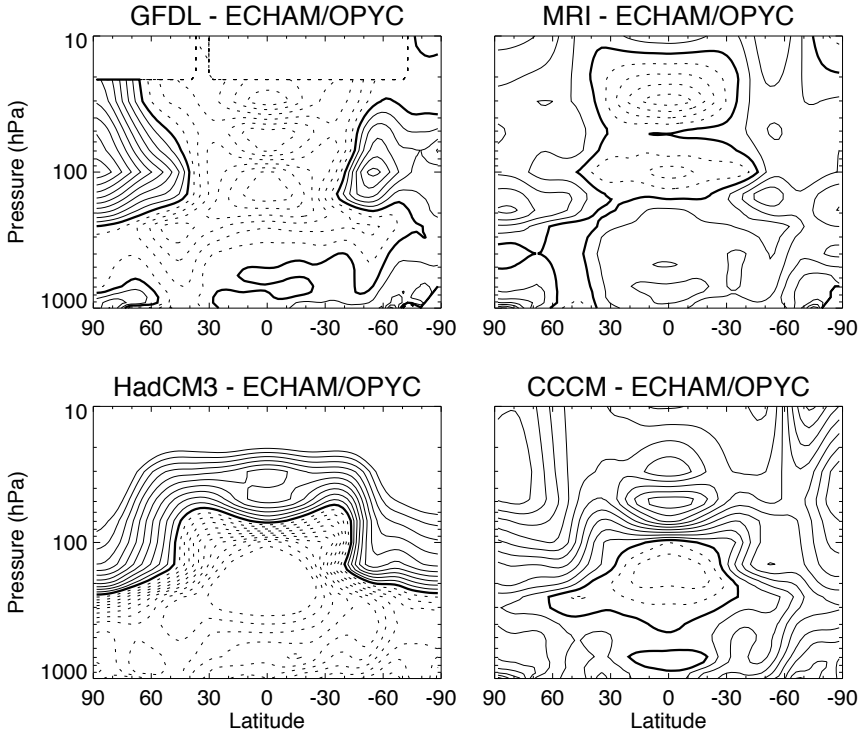

Fig. 3. Difference in zonal average temperature trends in five CMIP2+ models. These plots show the difference in zonal average temperature trends as simulated by five CMIP2+ models when subjected to increasing carbon dioxide at 1% yr^{-1}. The reference model is ECHAM4/OPYC3. The other models are those of GFDL (upper left), MRI (upper right), HadCM3 (lower left), and CCCM (lower right). Contour intervals are 0.05 K $decade^{-1}$. Solid (dashed) line contours are for positive (negative) values, and the thick line is the zero contour.

model (CSIR Mk2); the Japanese Meteorological Research Institute (MRI, CGCM 2.3); the American Geophysical Fluid Dynamics Laboratory model (GFDL, version R30_c), NCAR's Climate System Model (CSM, version 1), and Parallel Computing Model (PCM, run B04.30); and Canadian Climate Centre Model (CCCM, version 2). Each of these models was subjected to increasing carbon dioxide at 1% yr^{-1}, about twice the rate of recent history.

The models of CMIP2+ show considerable disagreement in their predictions of atmospheric trends when subjected to the same forcing. Fig. 3 shows the zonal average difference of temperature trends of four models in comparison and that of ECHAM4/OPYC3. In all models, the stratosphere cools but with different patterns and in different amounts. The best agreement is between ECHAM4/OPYC3 and MRI, but even this comparison has interesting

differences. While the amount of stratospheric cooling integrated over area is the same for these two models, the pattern shows enhanced cooling in MRI relative to ECHAM4/OPYC3 in the tropics and vice versa in the extratropics. This is the signature of the stratospheric Brewer-Dobson circulation increasing in strength more rapidly in the MRI model than in ECHAM4/OPYC3: upward (downward) motion in the tropics causes adiabatic expansion (compression) and cooling (warming) when the Brewer-Dobson circulation is strengthened. The GFDL model shows similar trends in the stratosphere with respect to ECHAM4/OPYC3 as does MRI but with a much greater difference in the Brewer-Dobson circulation strength. Both HadCM3 and CCCM show substantially less stratospheric cooling in an increasing carbon dioxide experiment than ECHAM4/OPYC3.

The Brewer-Dobson circulation is a residual mean circulation induced by the deposition of vertically propagating planetary waves originating in the troposphere [13]. If the Brewer-Dobson increases in strength, it necessarily means that more planetary waves propagate vertically from the troposphere into the stratosphere. In turn, these planetary waves are generated by flow over topography and baroclinic and barotropic instability in the troposphere. The stratospheric tropical-extratropical temperature patterns in Fig. 3 gives information on the efficiency with which planetary waves are generated in the troposphere.

The difference in temperature trends in Fig. 3 also reveals fundamental tropospheric differences. The tropical tropospheric pattern of temperature trends of MRI less ECHAM4/OPYC3 reveals a Hadley circulation growing stronger with time in MRI than in ECHAM4/OPYC3. In the CCCM-ECHAM4/OPYC3 comparison, CCCM shows evidence of the tropopause increasing more rapidly in time than does ECHAM4/OPYC3. These differences can be related to the models' different mechanisms pertaining to the hydrological cycle.

The CMIP2+ models contributed output of temperature, geopotential height, and specific humidity, making it possible to simulate trends in microwave refractivity in a 1% yr^{-1} carbon dioxide experiment. Recall that microwave refractivity N is empirically determined to be

$$N = (n-1) \times 10^6 = a\,(\frac{p}{T}) + b\,(\frac{p_{\mathrm{W}}}{T^2}) \tag{5}$$

where n is the microwave index of refraction, p, T, and p_{W} are atmospheric pressure, temperature, and water vapor pressure, and the coefficients a and b are 77.6 K hPa^{-1} and 373.0×10^3 K^2 hPa^{-1}. Microwave refractivity integrated vertically as a function of height is an ideal observeable for climate monitoring [14]. It can be thought of as a "dry" pressure: above the mid-troposphere, increasing dry pressure can be interpreted as thermal expansion of the underlying atmosphere, and below the mid-troposphere increasing dry pressure can be interpreted as a combination of thermal expansion of the un-

derlying atmosphere and increasing precipitable water vapor in the overlying atmosphere.

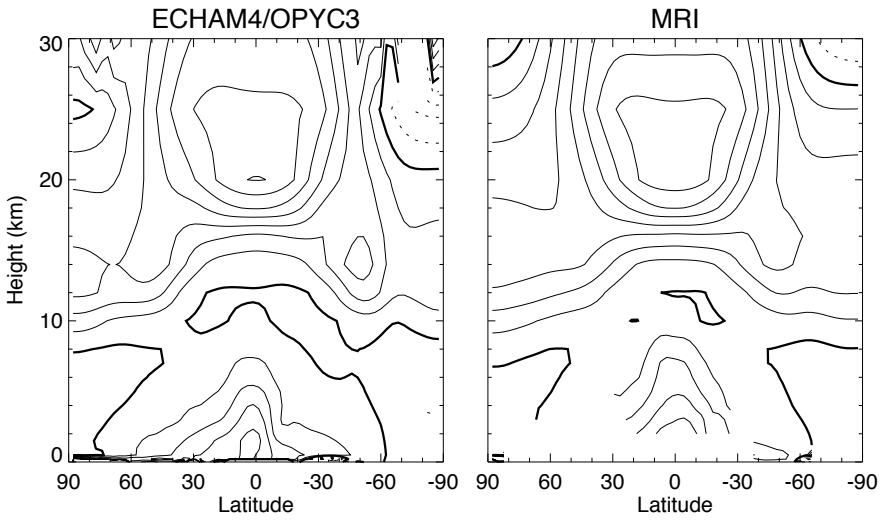

Fig. 4. Trends in microwave refractivity as simulated by the ECHAM4/OPYC3 and MRI climate models. The trends in zonal average microwave refractivity as a function of latitude and geopotential height as computed by 1% yr^{-1} carbon dioxide forced runs of the ECHAM4/OPYC3 and MRI climate models. Contour intervals are 0.1%. Solid (dashed) line contours are for positive (negative) trend values, and the thick line is the zero contour.

First, Fig. 4 shows the trends in microwave refractivity as produced by forced runs of two of the CMIP2+ climate models. Except for the tropical lower troposphere, much of the troposphere shows little trend in microwave refractivity despite the presence of tropospheric warming. This is explained by the fact that, while temperatures are increasing, pressure as a function of geopotential height is also increasing. The overall effect on density is one of cancellation, and since the "dry" component of refractivity is proportional to density, only a trend of less than 0.1% $decade^{-1}$ is seen throughout much of the troposphere.

The trend in integrated microwave refractivity conveys the notion of tropospheric warming better than trends in refractivity alone (see Fig. 5). As mentioned before, integrated refractivity is the same as pressure in the stratosphere and upper troposphere. A fractional change in pressure at a fixed height multiplied by a scaleheight is the same as the change in height of a constant pressure surface. For example, the maximum trend in integrated refractivity according to the MRI model is 0.6% $decade^{-1}$, which corresponds to an in-

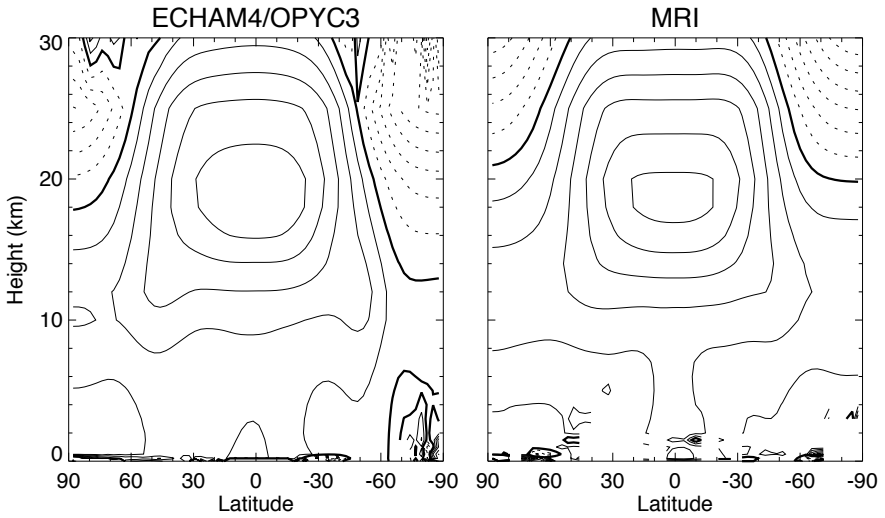

Fig. 5. Trends in microwave integrated refractivity as simulated by the ECHAM4/OPYC3 and MRI climate models. The trends in zonal average integrated microwave refractivity as computed by 1% yr^{-1} carbon dioxide forced runs of the ECHAM4/OPYC3 and MRI climate models are contoured as a function of latitude and geopotential height . Contour intervals are 0.1%. Solid (dashed) line contours are for positive (negative) trend values, and the thick line is the zero contour.

crease of the 100-hPa surface of 0.6% of a scaleheight per decade, or ≈ 30 m. The noisy output of the MRI model in the lowest layers of the troposphere is a reflection of the MRI model having an overly variable surface pressure field. The decrease of the integrated refractivity trend with increasing height above the tropopause is the signature of stratospheric cooling.

The relationship between water vapor increase and tropical tropospheric warming can be used to estimate the strength of the water vapor-longwave radiation feedback. If this feedback controls tropical tropospheric warming, then the rate of tropospheric expansion and lower tropospheric water vapor ought to be related by a constant factor. Tropospheric expansion can be estimated by the trend in integrated refractivity near the 16-km height level in the tropics, and water vapor from the refractivity trend in the tropical lower tropospheric refractivity trend. The constant factor can be deduced from a feedback analysis wherein the longwave radiation is made independent of water vapor anomalies [15, 16].

Observing trends in integrated microwave refractivity will strongly constrain the responses of the Brewer-Dobson circulation, the tropical hydrological cycle, and the poleward migration of the midlatitude storm track to increasing greenhouse gases (see Fig. 6). The MRI climate model shows

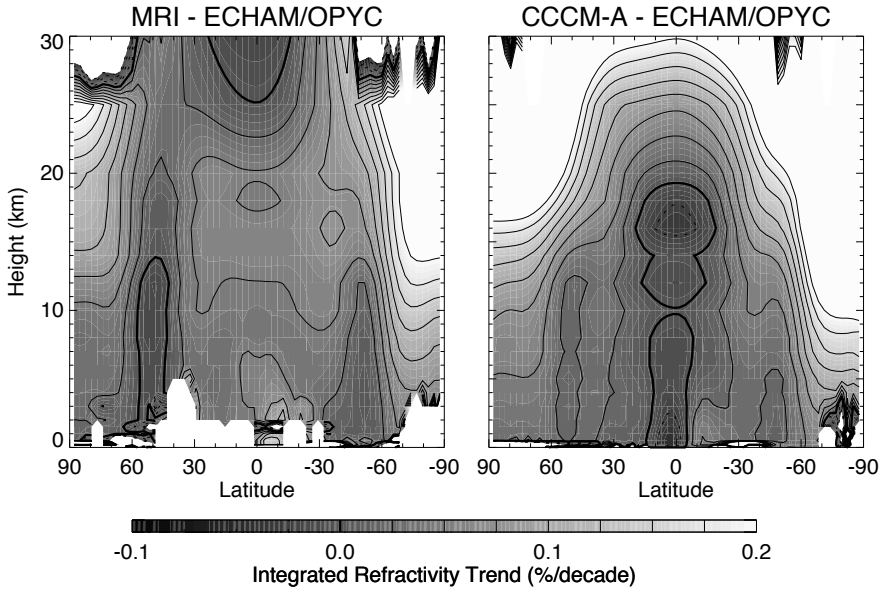

Fig. 6. Difference between model-forecast trends of integrated microwave refractivity. These plots show the difference between the forecast trends of integrated microwave refractivity from different models when each is forced by carbon dioxide increasing at 1% yr^{-1}. The plot on the left shows the difference between MRI and ECHAM4/OPYC3 model trends, and the plot on the right shows the difference between the CCCM and ECHAM4/OPYC3 model trends. The scale below the plots shows the contours used in plotting.

integrated refractivity (approximately pressure at constant height/height at constant pressure) increasing slower than ECHAM4/OPYC3 at low latitudes and faster at high latitudes in the stratosphere. This is the signature of the Brewer-Dobson circulation increasing faster according to MRI than according to ECHAM4/OPYC3. Temperature trends and integrated refractivity reveal this because an accelerated Brewer-Dobson circulation implies warming of the stratosphere at high latitudes and cooling at low latitudes, which means heights of constant pressure surfaces increase at high latitudes and decrease at low latitudes. In the tropical troposphere, the difference in humidity trends between models that climate monitoring with GPS occultation yields information on the hydrological cycle which can be used to improve our forecasting ability of it. Finally, the ridges in integrated refractivity/pressure trends seen at 50°N and S in the troposphere indicate sensitivity to the midlatitude storm track position. Such a ridge comes about because the storm track migrates northward in response to forcing by increasing carbon dioxide. In this exam-

ple, the MRI model shows much more rapid poleward migration of the storm track than ECHAM4/OPYC3 as does CCCM, yet CCCM less so.

Table 1. Science requirements for climate monitoring with GPS occultation. GPS occultation has clear sensitivity useful for improving forecasting ability of the phenomena listed below. The accuracy is given in units of a percentage of microwave refractivity. The temporal resolution required for each phenomenon is seasonal. The ITCZ is the intertropical convergence zone.

Phenomenon	Accuracy	Spatial resolution
Brewer-Dobson circulation	0.2% in stratosphere	hemispherical, scaleheight
Hydrological cycle	0.01% in troposphere	ITCZ, ~ 4 km
Storm track	0.01% in troposphere	meridionally 5°, scaleheight

In order to deduce requirements for climate monitoring, one needs to know how long before a signal, such as that seen in Fig. 6, emerges above the background noise of natural interannual fluctuations of the climate. The calculation which needs to be performed is that described in the previous section wherein one defines the data $\mathbf{d}$ to be the Jacobian $\nabla_\mu \mathbf{f}$ and finding the amount of time required before $|\mathbf{\Sigma}_{\mu,\mathrm{mp}}| \ll |\mathbf{\Sigma}_\mu|$. This is the requirement for Bayesian learning, i.e. when significant improvements can be made in our estimates of the model's parameters. If we assume that a strong test can be performed in two decades, corresponding to a growth in carbon dioxide concentration of approximately 10%, we can derive approximate requirements for climate monitoring using GPS occultation. Those numbers correspond to the decadal response of the climate models forced by 1% yr^{-1} in the CMIP2+ perturbed runs. They are enumerated in Table 1.

4 Benchmarking GPS Occultation

We have arrived at scientific requirements for monitoring climate using GPS occultation predicated on the assumption that we must learn something about the climate in the process of monitoring it. But what do these requirements mean in practice? What kind of monitoring system is needed? How must the data be processed? The solution must satisfy the needs of a future user who will difference data sets widely separated in time to detect meaningful trends in the climate system over that time. The solution is to make GPS occultation a *benchmark* measurement. A key component of making a benchmark measurement lies in the methodology of making climate monitoring traceable to the international system of units, otherwise known as "S.I. traceability."

GPS occultation has claimed absolute accuracy for years, but it is not really absolutely accurate. But how accurate can it be made? The Système

International d'Unités (International System of Units, international abbreviation S.I.) provides a recommended system of metrological units with well-determined uncertainties ideally suited to assessing the accuracy of physical measurements. The primary realizations of the S.I. base units provide the most accurate foundation possible for measurements made in the most familiar physical units: the second, the meter, the kilogram, the ampere, the kelvin, the candela and the mole. For example, if one wants to measure the mass of an object, the most accurately it can ever be done is by use of the S.I. prototype kilogram as a counterweight and collecting enough information on the balance system to remove as many potential systematic errors as possible. This technique of calibration, which has a clear relationship between the S.I. foundation and the presented measurement, has demonstrable "S.I. traceability" [17].

In the case of GPS occultation, much of the work in guaranteeing S.I. traceability has already been done. The Doppler delay of the GPS signal induced by the atmosphere is the basic measurement in a GPS occultation (which can be turned into refractivity profiles in retrieval), and, hence, GPS occultation is a timing measurement. Guaranteeing S.I. traceability means tying the atmospheric Doppler delay to the international standard for the second. This is done through the double-difference methodology of processing GPS occultation [18, 19], wherein the atmospheric path delays can be calibrated by Cs-133 atomic clocks [20] by measuring phase to a reference GPS satellite during an occultation event and observing both the occulting and reference GPS satellites with an atomic clock on the ground. Even if the atomic clock on the ground is not directly traceable to a Cs-133 clock, S.I. traceability is maintained as long as the ground atomic clock has been calibrated against the Cs-133 clocks with accuracy sufficient for radio occultation.

Even with double-differencing, hurdles remain in tracing a GPS occultation to the international definition of the second. These hurdles include (but are not limited to) unusual ionospheric activity and uncertainties in GPS and receiver spacecraft orbits. While GPS ordinarily provides two frequencies for the removal of ionospheric effects, it is possible for the ionosphere to become so active that its effects on occultation cannot be completely removed using the two GPS frequencies. To maintain S.I. traceability, it becomes necessary to collect information on the ionosphere sufficient to compensate for this unwanted noise or sufficient to know when an occultation cannot be used. In addition, bending angles in GPS occultation can only be found with precise information on the orbits of the GPS and receiver satellites. The orbits themselves are determined only after assumptions are made on the impact of the exosphere on the satellites' orbits, making the orbit solutions untraceable to S.I. standards. To maintain S.I. traceability, it is necessary to not only archive the satellites' precise orbit solutions, but also the occultation receiver measurements of phase to overhead GPS satellites and the measurements of GPS phase by reference ground networks used in the determination of precise orbits.

Creation of a benchmark measurement requires an archive of the S.I. traceable observations and external information on physical properties of potential error, but not a perfectly accurate retrieval algorithm. As long as an archive of the S.I. traceable components exists for all time, any potential future user will have enough information to implement his own retrieval algorithm. The investigator would use the same retrieval algorithm for every occultation data set, and this guarantees the consistency required for evaluating trends in the climate system over long time baselines. In GPS occultation, the data required to make it a benchmark measurement are

- atmospheric phase delay as a function of time as calibrated by the double-differencing methodology,
- the Keplerian orbital elements as a function of time used to deduce the bending of the occultation signal by the atmosphere,
- the ground station and receiver satellite phase measurements used in the calculation of orbits, and
- data on the activity of the ionosphere in the vicinity of the occultation, especially activity related to ionospheric turbulence.

The platforms exist to collect and archive the information of the first three items, but not the fourth item. This points to the necessity of tracking global scale ionospheric activity in the form of a scalar as a function of time and possibly deploying an ionospheric monitoring system which can map ionsopheric activity as a function of space and time in the lower ionsophere.

Acknowledgments. We thank the contributors to CMIP2+ for making the outputs of forced runs of their models available to us for analysis.

References

1. L.L. Yuan, R.A. Anthes, R.H. Ware, C. Rocken, W.D. Bonner, M.G. Bevis, and S. Businger. Sensing climate-change using the Global Positioning System. *J. Geophys. Res.*, 98(D8):14925–14937, 1993.
2. W.G. Melbourne, E.S. Davis, C.B. Duncan, G.A. Hajj, K.R. Hardy, E.R. Kursinski, T.K. Meehan, L.E. Young, and T.P. Yunck. The application of spaceborne GPS to atmospheric limb sounding and global change monitoring. Technical Report 94-18, Jet Propulsion Laboratory, California Institute of Technology.
3. E.R. Kursinski, G.A. Hajj, J.T. Schofield, R.P. Linfield, and K.R. Hardy. Observing Earth's atmosphere with radio occultation measurements using the Global Positioning System. *J. Geophys. Res.*, 102(D19):23429–23465, 1997.
4. J.T. Houghton, Y. Ding, D.J. Griggs, M. Noguer, P.J. van der Linden, X. Dai, K. Maskell, and C.A. Johnson, editors. *Climate Chance 2001: The Scientific Basis, Contribution of Working Group I to the Third Assessment Report of the Intergovernmental Panel on Climate Change.* Cambridge University Press, New York, 2001.

5. C.K. Folland, T.R. Karl, and Coauthors. *Climate Chance 2001: The Scientific Basis, Contribution of Working Group I to the Third Assessment Report of the Intergovernmental Panel on Climate Change*, chapter Observed Climate Variability and Change, pages 99–181. In Houghton et al. [4], 2001.
6. E. Kalnay, M. Kanamitsu, R. Kistler, W. Collins, D. Deaven, L. Gandin, M. Iredell, S. Saha, G. White, J. Woollen, Y. Zhu, M. Chelliah, W. Ebisuzaki, W. Higgins, J. Janowiak, K.C. Mo, C. Ropelewski, J. Wang, A. Leetmaa, R. Reynolds, R. Jenne, and D. Joseph. The NCEP-NCAR Reanalysis Project. *Bull. Amer. Meteor. Soc.*, 77(3):437–471, 1996.
7. H. Douville, F. Chauvin, S. Planton, J.F. Royer, D. Salas-Melia, and S. Tyteca. Sensitivity of the hydrological cycle to increasing amounts of greenhouse gases and aerosols. *Climate Dyn.*, 20(1):45–68, 2002.
8. R. Goody, J. Anderson, and G. North. Testing climate models: An approach. *Bull. Amer. Meteor. Soc.*, 79(11):2541–2549, 1998.
9. S.S. Leroy. Detecting climate signals: Some Bayesian aspects. *J. Climate*, 11(4):640–651, 1998.
10. P.A. Stott, S.F.B. Tett, G.S. Jones, M.R. Allen, W.J. Ingram, and J.F.B. Mitchell. Attribution of twentieth century temperature change to natural and anthropogenic causes. *Climate Dyn.*, 17(1):1–21, 2001.
11. C.E. Forest, P.H. Stone, A.P. Sokolov, M.R. Allen, and M.D. Webster. Quantifying uncertainties in climate system properties with the use of recent climate observations. *Science*, 295(5552):113–117, 2002.
12. C. Covey, K.M. AchutaRao, U. Cubasch, P. Jones, S.J. Lambert, M.E. Mann, T.J. Phillips, and K.E. Taylor. An overview of results from the Coupled Model Intercomparison Project. *Global and Planetary Change*, 37(1–2):103–133, 2003.
13. P.H. Haynes, C.J. Marks, M.E. McIntyre, T.G. Shepherd, and K.P. Shine. On the downward control of extratropical diabatic circulations by eddy-induced mean zonal forces. *J. Atmos. Sci.*, 48(4):651–679, 1991.
14. S.S. Leroy and G.R. North. The application of COSMIC data to global change research. *Terr. Atmos. Ocean. Sci.*, 11(1):187–210, 2000.
15. A. Hall and S. Manabe. The role of water vapor feedback in unperturbed climate variability and global warming. *J. Climate*, 12(8):2327–2346, 1999.
16. A. Hall and S. Manabe. Effect of water vapor feedback on internal and anthropogenic variations of the global hydrologic cycle. *J. Geophys. Res.*, 105(D5):6935–6944, 2000.
17. D.B. Pollock, T.L. Murdock, R.U. Datla, and A. Thompson. Data uncertainty traced to SI units. Results reported in the International System of Units. *Int. J. Rem. Sensing*, 24(2):225–235, 2003.
18. K.R. Hardy, G.A. Hajj, and E.R. Kursinski. Accuracies of atmospheric profiles obtained from GPS occulations. *Int. J. Sat. Comm.*, 12(5):463–473, 1994.
19. G.A. Hajj, E.R. Kursinski, L.J. Romans, W.I. Bertiger, and S.S. Leroy. A technical description of atmospheric sounding by gps occultation. *J. Atmos. Solar Terr. Phys.*, 64(4):451–469, 2002.
20. Bureau International des Poids et Mesures, Paris. *The International System of Units*, 7 edition, 1997.